Materials Science in Semiconductor Processing 167 (2023) 107796

Contents lists available at ScienceDirect

Materials Science in Semiconductor Processing

journal homepage: www.elsevier.com/locate/mssp

Generation and loss of hydrogen-boron pairs in fired silicon wafers

V.V. Voronkov *, R. Falster

Global Wafers, via Nazionale 59, 39012, Merano Italy

ARTICLE INFO

Keywords:
Silicon
Hydrogen
Boron
Diffusion

ABSTRACT

A dark anneal of fired B-doped samples is known to generate HB pairs which is followed by a loss of HB upon a prolonged anneal. In this paper, the reported data on the evolution of the total concentration of free and trapped ions, $C = [H^+] + [HB]$ (with a dominant contribution of HB) are used to extract the model parameters α (the dissociation coefficient of quenched-in hydrogen dimers, H_{2A}), χ (the constant relating $[H_{2A}]$ and [HB] under equilibrium), β (the kinetic coefficient for the production of stable dimers, H_{2C}). A loss of HB can be caused also by hydrogen out-diffusion; the computed diffusion-limited loss, surprisingly, is well faster than the observed loss. The reasons for this discrepancy are discussed. One possibility is that the hydrogen is trapped by boron initially into a metastable state with subsequent transformation into a stable state, of a lower effective diffusivity. This concept is supported by a peculiar evolution of [HB] observed under room-temperature illumination.

1. Introduction

Fabrication of solar cells often involves a firing step [1] with a peak temperature around 800 °C. This treatment leads to incorporation of hydrogen from a hydrogen-rich surface nitride layer; the incorporated hydrogen concentration [2] can be as large as 3×10^{15} cm^{-3}. It was long recognized [3,4] and recently confirmed [5] that the presence of hydrogen is vital for recombination properties of solar cells.

In the as-fired state, hydrogen is represented [2,6] mostly by neutral dimers (interstitial molecules) labeled H_{2A}. Subsequent dark annealing of boron-doped wafers, in a range 140–290 °C, leads to generation of hydrogen-boron pairs HB at a rate proportional to the hole (boron) concentration [6]. The whole reaction sequence is then: 1) a hole-assisted dissociation of dimers ($H_{2A} + h^+ \rightarrow H^+ + H^0$), 2) recharging of neutral atoms H^0 into H^+, 3) reversible trapping of H^+ by boron into neutral pairs HB. The free ions H^+ and the trapped ions HB coexist in the equilibrium relation:

$$[H^+][B^-] / [HB] = K, \tag{1}$$

where $[B^-]$ is the concentration of remaining (non-passivated) boron and K is the equilibrium dissociation constant. A value of K has been specified [7] but it requires some refinement (see section 3). At a representative temperature of 160 °C, K is close to 1.5×10^{14} cm^{-3}. Normally, the boron acceptor concentration $[B^-]$ is much larger than K. By Eq. (1), this means that $[H^+] \ll [HB]$. Although H^+ is a minor fraction of total hydrogen, it plays the major role in hydrogen effects since highly mobile hydrogen ions H^+ (and the related neutral species H^0) can react with various defects modifying their recombination activity.

Generation of neutral HB pairs means a partial passivation of boron acceptors; the remaining acceptor concentration is $[B^-] = N_B - [HB]$ where N_B is the total boron concentration (doping level). The hole concentration p is reduced mostly by passivation, and also due to H^+ donors:

$$p = N_B - [HB] - [H^+]. \tag{2}$$

In the total concentration of trapped and free ions, $C = [HB] + [H^+]$, a small contribution of H^+ will be preserved because it may become appreciable at higher T when $K(T)$ becomes larger (the activation energy for $K(T)$ is estimated as 0.71 eV in Section 3).

A simple technique [8] to determine the time evolution curve $[HB](t)$ (more precisely, $C(t)$) is to measure the specific resistivity and convert it to the hole concentration $p(t)$; then C is found as $N_B - p$.

The reported evolution of [HB] during dark annealing [2,6] involves an initial rise in [HB] due to a conversion of H_{2A} into HB. The kinetic equation for this process [9] reads

$$d[H_{2A}]/dt = -\alpha p \left([H_{2A}] - \chi [HB]^2 / (p [B^-])^2\right), \tag{3}$$

where α is the kinetic coefficient for dissociation of H_{2A} and χ is the equilibrium constant for the exchange between H_{2A} into HB. Upon annealing, $[H_{2A}]$ gradually approaches the equilibrium value

* Corresponding author.
E-mail address: vvoronkov@gw-semi.com (V.V. Voronkov).

https://doi.org/10.1016/j.mssp.2023.107796
Received 11 May 2023; Received in revised form 7 August 2023; Accepted 9 August 2023
Available online 18 August 2023

corresponding to a zero right-hand part of Eq. (3).

A subsequent prolonged annealing leads to a slow reduction in [HB], presumably [9] by formation of stable dimers labeled H_{2C}. This pairing reaction is assumed to be $H^+ + HB \rightarrow H_{2C} + B^- + 2\,h^+$ (generating two holes), and then the pairing rate is

$$d[H_{2C}]/dt = \beta\,[HB]^2\,/\,[B^-], \tag{4}$$

where β is the kinetic pairing coefficient. If the back reaction, from H_{2C} to HB, were included, the final equilibrium relation between HB and H_{2C} would be similar to that between HB and H_{2A} in Eq. (3). The estimated value of the corresponding equilibrium constant (χ_C) is so high [9] that the final concentration of HB, equal to $p\,[B^-]\,([H_{2C}]/\chi_C)^{0.5}$, is negligible provided that $[B^-]$ is well smaller than 10^{17} cm^{-3}. In that case, [HB] tends to zero upon prolonged annealing.

The concentration C is expressed through $[H_{2A}]$ and $[H_{2C}]$ since the total hydrogen concentration, $C_T = C + 2[H_{2A}] + 2\,[H_{2C}]$, remains constant (if, at the moment, out-diffusion loss of hydrogen is neglected). A drop in $[H_{2A}]$ by Eq. (3) means generation of HB, and a rise in $[H_{2C}]$ by Eq. (4) means a loss of HB.

Simulation of the $C(t)$ and [HB](t) curves by Eqs. (3) and (4) requires four fitting parameters: three constants (α, β, χ) and the total hydrogen concentration C_T. These parameters have been determined [2] in a range of annealing temperature. The deduced coefficients α(T) and χ(T) were remarkably scattered, and only scarce values for β(T) were obtained. Recently, more $C(t)$ curves were reported [10–13], and the aim of the present paper is to use this expanded database to get more points for the temperature dependence of the relevant parameters α, χ and especially β. With the added points, the Arrhenius-type temperature dependence of these parameters becomes more persuasive.

2. Fitting the experimental curves $C(t)$

Prior to applying the fitting procedure, it should be noted that the hydrogen concentration in fired samples is dependent on the depth coordinate z. The diffusivity of atomic hydrogen [14] is about 5×10^{-5} cm^2/s at 800 °C – enough to diffuse to more than a sample half-thickness during several seconds spent near the peak firing temperature. At this stage, the hydrogen depth profile is almost uniform; the concentration corresponds to the solubility from the nitride layer. During subsequent ramp down, the solubility decreases resulting in a significant out-diffusion; a final (as-fired) depth profile will be of a sinusoidal shape. The experimentally determined hole concentration is the average of $p(z)$ over the depth. Accordingly the deduced concentration C represents the average of $C(z)$. In a simplified version, we replace the actual depth profile of each hydrogen species by a uniform profile of the same average concentration. The kinetic equations (3) and (4) are applied to these uniform profiles. In the subsequent sections, also evolution of the depth profiles will be considered.

To solve the kinetic equations, one needs a relation between [HB] and $C = [HB] + [H^+]$ which follows from Eq. (1):

$$C = [HB] + K\,[HB]\,/\,(N_B - [HB]). \tag{5}$$

With a specified C, the HB concentration is calculated by this equation.

In ref. [10], the fired wafers were annealed at 220 °C to provide $C(t)$ curves with well pronounced rise and loss parts (Fig. 1). The wafers strongly differ in the maximum concentration of $C(t)$ – and hence in the incorporated hydrogen concentration C_T - due to different peak temperatures of firing, 730–855 °C. In Fig. 1 four representative curves are shown.

By fitting a $C(t)$ curve, only 3 parameters out of 4 can be reliably deduced. If the parameter χ is fixed – within a range estimated in Ref. [2] – then the other fitting parameters do not depend much on the assumed value of χ which is chosen to be 2×10^{49} cm^{-9}. The deduced concentration C_T ranges from 4.6×10^{14} to 2.1×10^{15} cm^{-3}. The kinetic coefficient α is almost the same for all the curves, about 1.6×10^{-20} cm^3/s,

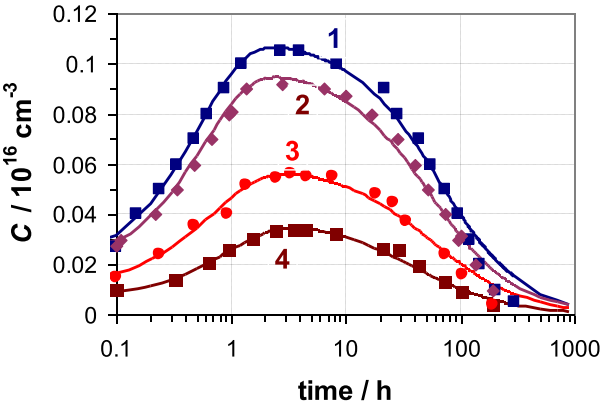

Fig. 1. Evolution of the total concentration $C = [HB] + [H^+]$ of trapped and free hydrogen ions at 220 °C for fired nitride-coated samples ($N_B = 1.5 \times 10^{16}$ cm^{-3}) by Ref. [10]. The curves 1 to 4 are for different peak temperatures of firing. The solid curves are best-fits by Eqs. (3) and (4).

and β is in a range $(0.7–2)\times10^{-4}$ s^{-1}.

Another set of wafers [10] was bare (without nitride layer), fired under fixed conditions but annealed at various T. The evolution of C (Fig. 2) was of the same type as before, only with a smaller maximum value. This shows that even bare wafers can contain an appreciable amount of hydrogen that can be incorporated from the surface prior to firing. The effect of firing is to spread the hydrogen over the depth and to create H_{2A} upon a quench. At the lowest annealing temperature (200 °C), the assumed value of χ does not affect much the deduced concentration C_T that was found to be 3.6×10^{14} cm^{-3}. With a specified C_T, the $C(t)$ curves for higher annealing temperatures give all the three coefficients including χ. In Fig. 2, the curves for 200, 220, 240 and 260 °C are shown; a reduction in the maximum concentration at a higher T is due to an increased χ and accordingly reduced fraction of HB in the equilibrated HB/H_{2A} community. At 220 °C, the deduced parameters α and β are similar to those extracted for the previous (nitride-coated) samples.

In ref. [11], the annealing temperatures (for fixed firing conditions of nitride-coated wafers) were 160, 200 and 220 °C. The curve for 160 °C

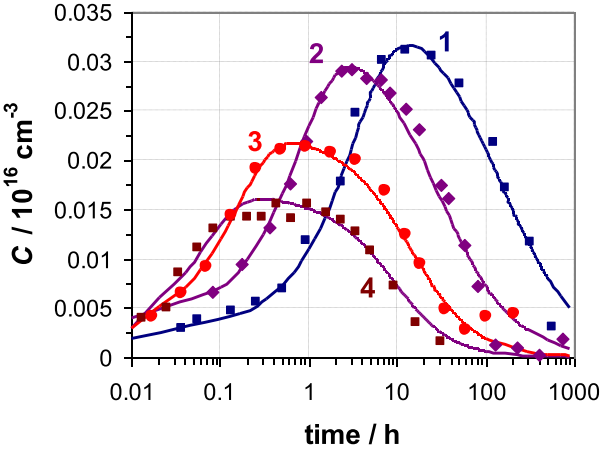

Fig. 2. Evolution of the total concentration C of trapped and free H^+ ions for fired bare (non-coated) samples ($N_B = 1.5 \times 10^{16}$ cm^{-3}) by Ref. [10]. The curves 1 to 4 are for different annealing temperatures: 200, 220, 240 and 260 °C, resp. The solid curves are best-fits by Eqs. (3) and (4).

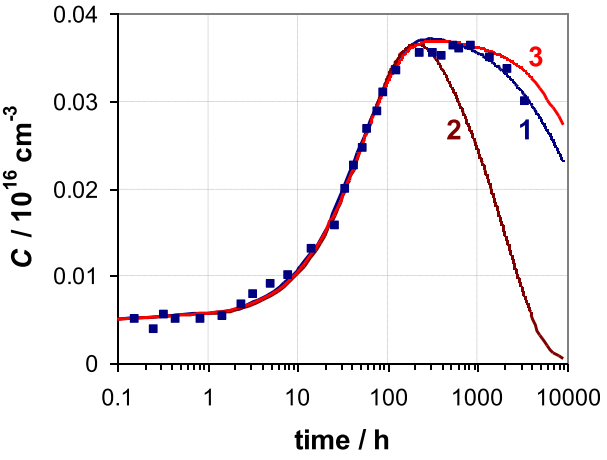

Fig. 3. Evolution of the concentration C at 160 °C for fired nitride-coated sample ($N_B = 1.7 \times 10^{16}$ cm^{-3}) by Ref. [11]. The solid curve 1 is the best-fit by Eqs. (3) and (4). The solid curves 2 and 3 are computed for a diffusion-limited loss of hydrogen with the dissociation constant $K = 1.5 \times 10^{14}$ and 10^{13} cm^{-3}, resp.; the sample thickness $d = 250$ μm.

(Fig. 3) is not sensitive to the assumed value of χ, and one can deduce $C_T = 3.8 \times 10^{14}$ cm^{-3}, $\alpha = 3 \times 10^{-6}$ cm^3/s and $\beta = 4.6 \times 10^{-7}$ s^{-1}. With a defined C_T, one can deduce α, β, χ at two higher T.

In ref. [12], a fired wafer was annealed at 160 °C (Fig. 4, curve 1). The deduced parameters are $C_T = 1.85 \times 10^{15}$ cm^{-3}, $\alpha = 2.5 \times 10^{-6}$ cm^3/s and $\beta = 4 \times 10^{-7}$ s^{-1}. The values of α and β are close to those found above. The curves 2 and 3 in Fig. 4 represent wafers annealed at 175 °C [13]. They were quenched from the same peak firing temperature (800 °C) but with a different rate: slow ramp down (curve 2, deduced $C_T = 1.8 \times 10^{15}$ cm^{-3}) and fast ramp down (curve 3, deduced $C_T = 3.75 \times 10^{15}$ cm^{-3}). A faster quench leads to a higher C_T. The kinetic parameters are almost the same for these two curves: $\alpha \approx 5.5 \times 10^{-22}$ cm^3/s and $\beta \approx 1.1 \times 10^{-6}$ s^{-1}.

The coefficients deduced above (open symbols), together with the previously defined values [2], filled symbols is displayed in Figs. 5–7.

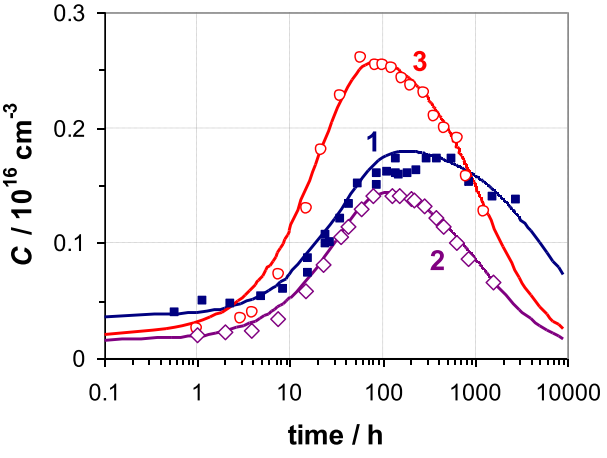

Fig. 4. Evolution of the concentration C for fired nitride-coated samples by Refs. [12,13]. The curve 1 is for annealing at 160 °C ($N_B = 3.2 \times 10^{16}$ cm^{-3}). The curves 2, 3 are for annealing at 175 °C ($N_B = 1.46 \times 10^{16}$ cm^{-3}) with a slow (curve 2) and fast (curve 3) ramp-down from the peak firing temperature of 800 °C. The solid curves are the best-fits by Eqs. (3) and (4).

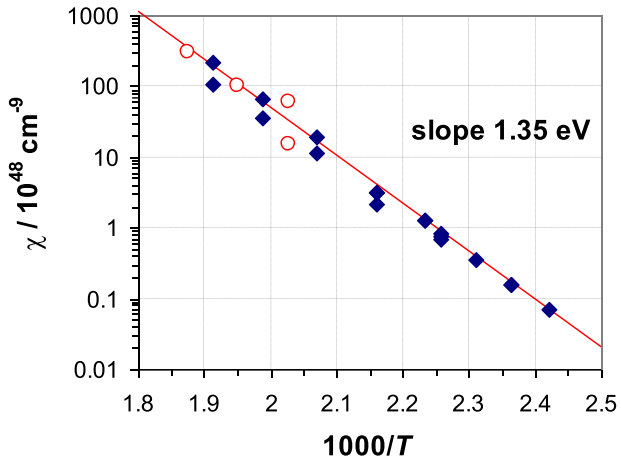

Fig. 5. Deduced values of the equilibrium constant χ. The filled symbols are previous data by Ref. [2], the open symbols are the added points by Refs. [10, 11]. The temperature T is in K.

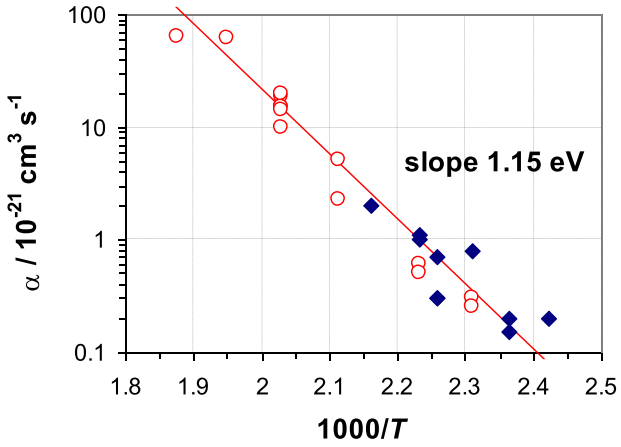

Fig. 6. Deduced values of the dissociation coefficient α of H_{2A} dimers. The filled symbols are previous data by Ref. [2], the open symbols are the added points by Refs. [10–13].

In the plot for the equilibrium constant χ (Fig. 5) only few points have been added. The value of χ at 200 °C is not shown since it is not considered reliable. On average, the points follow an Arrhenius-type temperature dependence with the activation energy of 1.35 eV.

The dissociation coefficient α (Fig. 6) is less scattered for the new points which makes the Arrhenius-type dependence more persuasive; the activation energy is 1.15 eV.

The temperature dependence of the pairing coefficient β (Fig. 7) is represented mostly by the added points that show, in spite of some scatter, an Arrhenius-type dependence; the activation energy is 1.9 eV. There is a strong variation in β at 220 °C correlated with the total concentration C_T. If a first-order loss kinetics is assumed (replacing the right-hand part of Eq. (4) with β* [HB]), the deduced values of β* show a small scatter, around 2.5×10^{-6} s^{-1}. However, the loss data for 160 °C show a small scatter with the second-order kinetics as assumed in Eq. (4) and much stronger scatter with the first-order kinetics. The reason for the difference is not yet clear.

The parameters for the average Arrhenius-type dependence (the lines

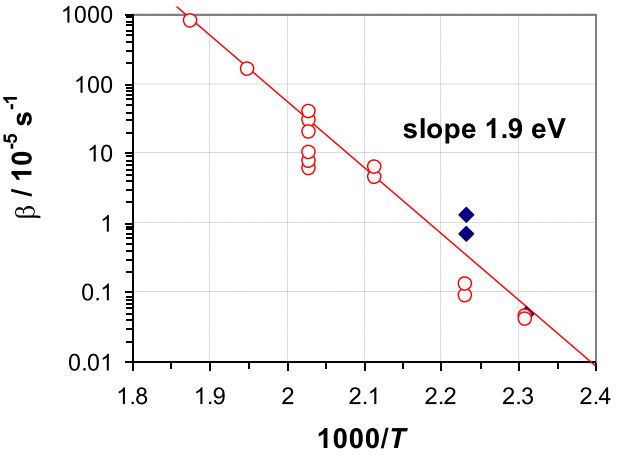

Fig. 7. Deduced values of the pairing coefficient β. The filled symbols are previous data by Ref. [2], the open symbols are the added points by Refs. [10–13].

in Figs. 5–7) are presented in Table 1.

3. Equilibrium dissociation constant for HB pair

The precise absolute value of the constant K in Eq. (1) was not essential in the previous analysis – for samples with $[B^-] \gg K$. However, it is important for some other considerations (see the next sections), and here we discuss a refined estimate for K.

In the first place, two independent kinds of hydrogen ions, $H^+(1)$ and $H^+(2)$ were concluded to exist [15] and to form two independent kinds of hydrogen-boron pairs, HB(1) and HB(2). The two subsystems differ in the value of D^+K product (D^+ is the ion diffusivity, $D^+(1)$ or $D^+(2)$) and in the behavior during dark annealing. The second subsystem, of a smaller D^+K, is irreversibly converted into some dimers [15,16]; this subsystem seems to be essential only under non-equilibrium conditions of plasma exposure. Then in samples subjected to a high-T treatment (including firing) we deal only with the first subsystem, $H^+(1)$/HB(1), for which H^+ is assumed to reside in a bond-centered position. The subsystem index (1) was omitted above, and will be omitted below.

The product D^+K was determined [7,15] by the depth profile of deuterium (^{2}H isotope) in plasma-exposed samples, to be about 5×10^4 cm^{-1} s^{-1} at 150 °C. The diffusivity D^+ for ^{1}H isotope can be expressed [17] through the measured re-orientation time of H^+ between the four different orientations of the bond-centered sites [18]. However the value for $D^+(T)$ claimed in Ref. [17] was later found [15] to be overestimated by a factor of four. The corrected diffusivity is

$$D^+ = (0.0001\ \mathrm{cm}^2/\mathrm{s})\ \exp(-0.43\ \mathrm{eV}\ /\ \mathrm{kT}). \quad (6)$$

For deuterium, it is smaller by the mass ratio factor $2^{1/2}$, and amounts to 5.4×10^{-10} cm^2/s at 150 °C. Accordingly, $K(150\ °C) = 9.3 \times 10^{13}$ cm^{-3}; this value should be the same for both isotopes. The prefactor in $K(T)$ is expected [7] to be a half of the lattice site density, and then

Table 1
Parameters for average Arrhenius-type temperature dependence of the basic model constants.

Quantity	Activation energy, eV	Prefactor
χ	1.35	1.9×10^{63} cm^{-9}
α	1.15	7.2×10^{-9} cm^{3}s^{-1}
β	1.9	7.4×10^{15} s^{-1}

$$K(T) = (2.5 \times 10^{22}\ \mathrm{cm}^{-3})\ \exp(-E\ /\ \mathrm{kT}), \quad (7)$$

where E is the binding energy of H^+ and B^-. By the absolute value of K (150 °C), $E = 0.71$ eV. The sum of the migration barrier (0.43 eV) and the binding energy (0.71 eV) is remarkably close to the reported [19] dissociation energy (1.28 eV) for HB.

By equations (6) and (7), $D^+(160\ °C) = 10^{-9}$ cm^2/s and $K(160\ °C) = 1.5 \times 10^{14}$ cm^{-3}.

4. Contribution of out-diffusion to a loss of HB

A loss of HB during a prolonged annealing (Figs. 1–4) was attributed to formation of stable dimers H_{2C}. Another possible reason for a loss can be out-diffusion of hydrogen, especially taking into account a small thickness d of the inspected wafers (150–250 μm). The hydrogen transport in p-Si is assumed to occur by diffusion of H^+ ions equilibrated with HB, neglecting a contribution of other charge states. The diffusion flux J is expressed [7] as

$$J = -D^+\ p\ \partial([H^+]/p)/\partial z, \quad (8)$$

taking into account a drift of H^+ in the electric field induced by a non-uniformity in p. For the sake of qualitative estimate, this expression can be simplified: in all the present samples, C is well smaller than the doping level N_B, and $p(z)$ is close to N_B. Upon replacing p with N_B, the flux becomes $J = -D^+\ \partial[H^+]/\partial z$. The concentrations $[H^+]$ and C are related by Eq. (1): $C = [H^+] + [HB] = [H^+]\ (1 + [B^-]/K)$ where again $[B^-]$ can be replaced with N_B. The simplified flux is then $J = -D^*\ \partial C/\partial z$ with an effective diffusivity $D^* = D^+K/(N_B + K)$ which is close to D^+K/N_B. The combination D^+K is equal to 1.5×10^5 cm^{-1} s^{-1} at 160 °C. For $N_B = 1.5 \times 10^{16}$ cm^{-3}, the effective diffusivity is $D^* = 10^{-11}$ cm^2/s. If the sample surface (both sides) were an ideal sink for H^+, the out-diffusion time, $(d/\pi)^2/D^*$, would be 1800 h in case of Fig. 3 ($d = 250$ μm) – well shorter than the time scale of the actual loss of HB.

A more precise treatment of out-diffusion is to solve the diffusion equation:

$$\partial C_T/\partial t = -\partial J/\partial z, \quad (9)$$

together with the kinetic Equations (3) and (4) for depth-dependent concentrations, using for the flux Eq. (8). To visualize the effect of out-diffusion on the loss of HB, the pairing reaction is now omitted ($\beta = 0$).

The initial profile of C_T is assumed sinusoidal: $C_T(z) = A\ \sin(\pi\ z/d)$. The amplitude A is related to the initial averaged value of C_T which is equal to $2A/\pi$.

The ideal sinking at the sample surfaces corresponds to the zero boundary condition for $C(z)$ at $z = 0$ and $z = d$.

The calculated $C(z, t)$ was averaged over the depth, and the averaged value is shown as the curve 2 in Fig. 3. As anticipated by a simplified approach, the calculated out-diffusion decay proceeds well faster than the actual decay. This astounding controversy can be understood if, in reality, the sample surface cannot accumulate hydrogen, at least in the present example (at 160 °C). This may be due to a high energy barrier for hydrogen incorporation into the surface layer.

Another explanation is that the HB species produced by trapping H^+ ions initially exist in a metastable configuration denoted HB(a), and later transform into a more stable configuration denoted HB(b). The dissociation constant K deduced above for plasma-exposed samples (for the time scale of about 1 h) is attributed to HB(a) – of a relatively small binding energy ($E = E_a = 0.71$ eV) and a relatively large value of the equilibrium dissociation constant ($K = K_a$). For a much longer annealing time of HB generation/loss, the primary metastable defects HB(a) are converted into HB(b), of a larger binding energy ($E = E_b$) and a much smaller value of $K = K_b$. The time scale of this conversion is assumed to be well shorter that the time to reach a maximum in $C(t)$, so that for the

most part of the $C(t)$ curve, the state of HB is HB(b). The effective diffusivity $D^* = D^+ K_b/N_B$ for this stable form is much smaller than the above estimate of D^* valid for HB(a). The out-diffusion loss of HB(b) proceeds much slower. The experimental curve in Fig. 3 is fitted with $K_b = 2 \times 10^{13}$ cm^{-3} which corresponds to $E_b = 0.78$ eV.

However the actual loss of HB cannot be attributed entirely to out-diffusion (dismissing a loss by pairing) since the rate constant for diffusion-limited loss is proportional to the effective diffusivity D^* and hence to $D^+ K_b$, with the activation energy of about 1.2 eV – well smaller than the activation energy of 1.9 eV found for the loss rate constant (Fig. 7). In our current opinion, the out-diffusion loss of HB can be neglected in the whole temperature range of Fig. 7, implying that K_b is sufficiently small. An insignificant loss by out-diffusion (in comparison to the actual loss) is found for $K_b = 10^{13}$ cm^{-3} (the curve 3 in Fig. 3) or for smaller K_b. For estimates, we adopt this upper limit, $K_b = 10^{13}$ cm^{-3}, which corresponds to $E_b = 0.81$ eV.

The equilibrium constants χ and K - for various kinds of hydrogen-acceptor pairs like HB(a) and HB(b) - are not independent. The concentrations of H^+ and H_{2A}, under equilibrium, are related by the mass action law

$$[H_{2A}] = Q\,([H^+]/p)^2. \tag{10}$$

The constant Q refers to the equilibrium between H_{2A} and H^+ and it is not related to trapping of H^+ by acceptors. By the equilibrium relation between H_{2A} and HB (zero right-hand part of Eq. (3)) together with Eq. (1), the equilibrium constant χ is found to be proportional to K^2:

$$\chi = Q\,K^2. \tag{11}$$

This relation, with the same value of the constant Q, is valid for all the kinds of hydrogen-acceptor pairs, whether HB(a), HB(b) or pairs involving other acceptors. By the values found at 160 °C ($\chi = 4 \times 10^{47}$ cm^{-9}, $K = 10^{13}$ cm^{-3} - ascribed to HB(b)) the constant Q is estimated to be 4×10^{21} cm^{-3}. With this number, the constant χ for HB(a) pairs ($K = K_a = 1.5 \times 10^{14}$ cm^{-3}) is calculated to be 9×10^{49} cm^{-9}.

5. Loss of HB by illumination at T_{room}

A concept of metastable and stable forms of the HB defect is supported by data [20] on the loss of HB induced by a room-temperature illumination. First, the HB defects were produced by a dark annealing at 175 °C for 30 h, to a concentration of 5.1×10^{14} cm^{-3}. Next, the sample was subjected to illumination of 1.7 sun at T_{room} for some hours (with occasional short interruptions to measure the resistivity), and then stored in the dark (overnight). This illumination-storage cycle was repeated several times.

The evolution of the concentration $C(t)$ is shown schematically in Fig. 8 (here, at T_{room}, C is identical to [HB] as all H^+ are trapped by boron). An initial time lag of about 3 h may be related to a yet insufficient electron concentration at this stage of illumination (the electron lifetime – remarkably degraded after the dark annealing - was found to be strongly increased upon increasing the illumination time [20]).

During the first cycle, [HB] was reduced by illumination by about 5×10^{13} cm^{-3} but almost completely restored to the initial value after a storage.

During the second cycle, the lost-and-restored concentration is lost again which occurs much faster than a loss of HB during the first cycle. After the storage, [HB] is increased but to a value distinctly smaller than the initial one. The subsequent cycles are not well resolved but similar to the second one.

Clearly, a loss of HB during the first cycle is not to H_{2A} since the H_{2A} dimers cannot be converted back into HB by a dark storage at T_{room}: the coefficient α extrapolated by Fig. 6 is negligible. Hence, the observed loss of HB is to a neutral monomer, H^0. This species is recharged to H^+ during a dark storage – when the excess electrons are no longer present. Then the H^+ are trapped by boron into HB. The trapping rate is $4\,\pi\,r\,D^+$ $[B^-]$ $[H^+]$ where r is the capture radius equal to $e^2/(\varepsilon\,kT)$ for Coulombic attraction of the reacting species (e is the elementary charge and ε is the dielectric constant). At T_{room}, $r = 5$ nm, and the trapping time, $1/(4\,\pi\,r\,D^+\,[B^-])$, is about 3 s which means a practically instantaneous trapping.

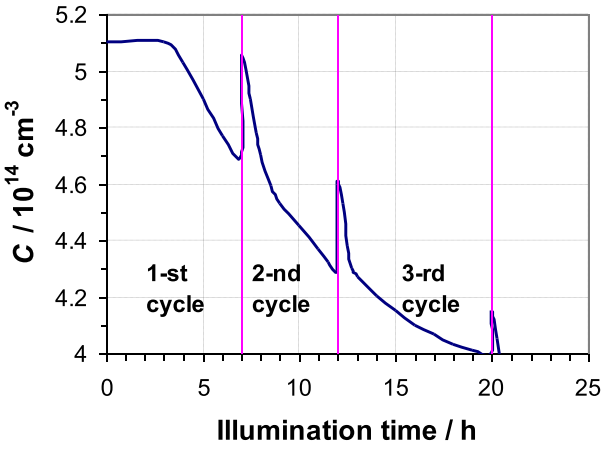

Fig. 8. Schematic evolution of [HB] (after [20]) induced by cycling of illumination and dark storage (both at T_{room}). Each storage is marked by a vertical line.

The initial state of HB pairs is HB(b) as the conversion time from HB (a) to HB(b) during dark annealing was assumed to be relatively short. But the HB produced by trapping of H^+ during the storage will be HB(a). At T_{room}, this metastable species is not reconfigured into HB(b). The population of HB defects after the first cycle is thus a mixture of HB(a) and HB(b). This nicely accounts for a quick decay in [HB] at the beginning of the second cycle (Fig. 8) if, under illumination (in the presence of excess electrons), a loss of the HB(a) defects occurs faster than a loss of the HB(b) defects.

An important feature of the room-temperature reactions is that even the metastable pair HB(a) has a very small rate constant for dissociation into H^+ and B^-. This rate constant is expressed [15] as $4\,\pi\,r\,D^+\,K$. With $K = K_a$, the dissociation time (inverse to the rate constant) is 300 h. The implication is that a loss of HB to H^0 is not by a two-step reaction (first dissociation of HB and then recharging of released H^+ into H^0 by excess electrons) but by a direct reaction of HB with electrons e^-:

$$HB + e^- \rightarrow B^- + H^0, \tag{12}$$

that occurs for both HB(a) and HB(b), with different rates. It appears [15] that there are several independent kinds of H^0, of different lattice location and of strongly different diffusivity. It can not be specified at the moment which one is produced by the reaction (12). More than that, the H^0 species originated from HB(a) may be different from that originated from HB(b). For the sake of simplicity, we will not consider this complication and assume that H^0 is the same for both reactions.

The produced H^0 species can be then trapped by HB(b) (to produce a neutral H_2B complex) or by the dominant impurities, oxygen and/or carbon. In that case, the time of dark conversion of neutralized hydrogen into H^+ – denoted τ_c – can be limited by de-tapping reaction, being quite long. To account for the evolution curve of Fig. 8, τ_c should be well longer than a short time interval used to measure the resistivity – to preserve the neutralized state. On the other hand, τ_c should be well shorter than the storage time – to ensure a conversion of trapped H^0 species into H^+ (with subsequent quick trapping into HB(a)). A direct way to deduce τ_c would be to monitor the resistivity during a storage but such data are missing.

The monoatomic hydrogen component (HB and H) is not lost during the first cycle but clearly lost during the second and subsequent cycles as

the restored [HB] (the peak concentration between the adjacent cycles) becomes progressively smaller (Fig. 8).

A simple explanation is that the hydrogen dimers are produced by a reaction involving HB(a) – the species that are absent during the first illumination step. This pairing reaction can be

$$HB(a) + H^- \rightarrow B^- + H_2. \quad (13)$$

This occurs under illumination - when H^0 is partially recharged into H^-. The produced H_2 dimers are presumably H_{2A}.

The overall change in the hydrogen state induced by illumination/storage cycles is from HB to H_2. A similar conversion was also found [21] under illumination at elevated T, after generation of HB by dark annealing. The kind of produced H_2 dimers was definitely H_{2A} since a subsequent dark annealing reproduced the evolution of [HB] observed during the initial dark annealing.

The H^0 species produced under illumination by the reaction (12) can be the reason for an interesting phenomenon [20]: a temporary recovery of degraded lifetime by illumination at T_{room}. The apparent recovery mechanism is a reaction of H^0 or H^- with the lifetime-degrading recombination centres.

6. Summary

The evolution of the HB concentration in fired samples, by dark annealing, includes two stages: 1) an initial rise due to conversion of quenched-in dimers H_{2A} into HB, 2) a subsequent slow loss of HB. One possible reason for the loss is a conversion of HB into stable dimers (H_{2C}). This model was adopted to fit the reported evolution curves $C(t)$ for the total concentration $[H^+]$ + [HB] of free and trapped hydrogen ions (with the major contribution of HB). The fitting constants are the kinetic coefficient α for the hole-assisted dissociation of H_{2A}, the equilibrium constant χ relating the concentrations of HB and H_{2A} in equilibrium, the kinetic pairing coefficient β for production of H_{2C}. The existing database allows to obtain many points in the temperature dependence of these constants. In spite of a considerable scatter, the overall temperature dependence is of an Arrhenius type.

Another reason for a long-time-scale loss of HB can be out-diffusion of hydrogen through minor but highly mobile H^+ species. Surprisingly, the calculated diffusion-limited loss of HB is remarkably faster than the observed loss. One explanation is that the sample surface does not act as a sink for hydrogen. Another – more sophisticated – model is that trapping of the H^+ ions by boron produces metastable pairs HB(a) which are later transformed into the stable configuration HB(b). For the latter pairs, the concentration of H^+ in equilibrium with HB is remarkable smaller, and the effective diffusivity is accordingly reduced.

At the moment, it is not clear which of the two explanations of a negligible (or slow) out-diffusion loss is valid. An experimental check of an out-diffusion contribution into the loss of HB would be to compare the $C(t)$ curves for samples that differ only in the thickness d (by thinning after firing) – of the same doping level and of the same firing conditions. With an appreciable contribution of out-diffusion, the loss of HB would be faster for a thinner sample.

A concept of two forms (HB(a) and HB(b)) of the HB defect is supported by the reported peculiar evolution of [HB] during illumination-storage cycles at T_{room}. Here the initially present stable pairs HB(b) seem to be transformed into neutral species H^0 along with H^- (during an illumination step) and then into metastable pairs HB(a) (during a storage). The H^0/H^- species may react with the recombination centres leading to a temporary lifetime recovery by illumination at T_{room}.

Author contribution

V.V.Voronkov: Conceptualization Original draft preparation, R.Falster: Writing, Reviewing, Editing.

Declaration of competing interest

The authors declare that they have no known competing financial interests or personal relationships that could have appeared to influence the work reported in this paper

Data availability

Only published data have been used

References

[1] R. Prue, E. Lochmuller, S. Lochmuller, P. Saint-Cast, J.M. Greulich, Appl. Phys. Rev. 7 (2020), 041315.
[2] D.C. Walter, V.V. Voronkov, R. Falster, D. Bredemeier, J. Schmidt, J. Appl. Phys. 131 (2022), 165702.
[3] S. Wilking, A. Herguth, G. Hahn, J. Appl. Phys. 113 (2013), 194503.
[4] B.J. Hallam, S.R. Wenham, P.G. Hamer, M.D. Abbott, Q.A. Sugianto, C.E. Chan, A. M. Wenham, M.G. Eadie, G. Xu, Energy Proc. 38 (2013) 561.
[5] L. Helmich, D.C. Walter, R. Falster, V.V. Voronkov, J. Schmidt, Sol. Energy Mater. Sol. Cells 232 (2021), 111340.
[6] R.E. Pritchard, J.H. Tucker, R.C. Newman, E.C. Lightowlers, Semicond. Sci. Technol. 14 (1999) 77.
[7] V.V. Voronkov, R. Falster, Phys. Status Solidi 214 (2017), 1700287.
[8] D.C. Walter, D. Bredemeier, R. Falster, V.V. Voronkov, J. Schmidt, Sol. Energy Mater. Sol. Cells 200 (2019), 109970.
[9] V.V. Voronkov, R. Falster, Phys. Status Solidi B 254 (2017), 1600779.
[10] C. Winter, J. Simon, A. Herguth, Phys. Status Solidi 2021 (2021), 2100220.
[11] Y. Acker, J. Simon, A. Herguth, Phys. Status Solidi 219 (2022), 2200142, 2022.
[12] B. Hammann, L. Rachdi, W. Kwapil, F. Schindler, M.C. Schubert, AIP Conf. Proc. 2487 (2021), 130004.
[13] B. Hammann, N. Assmann, P.M. Weiser, W. Kwapil, T. Niewelt, F. Schindler, R. Sondena, E.V. Monakhov, M.C. Schubert, IEEE J. Photovoltaics 13 (2023) 224.
[14] A. van Wieringen, N. Warmoltz, Physica 22 (1956) 849.
[15] V.V. Voronkov, Phys. Status Solidi 219 (2022), 2200981.
[16] T. Zundel, J. Weber, Phys. Rev. B 43 (1991) 4361.
[17] C. Herring, N.M. Johnson, C.G. Van de Walle, Phys. Rev. B 64 (2001), 125209-1.
[18] Y.V. Gorelkinski, N.N. Nevinnyi, Mater. Sci. Eng. B 36 (1996) 133.
[19] T. Zundel, J. Weber, Phys. Rev. B 39 (1989), 13549.
[20] W. Kwapil, B. Hammann, RRL Solar 2023 (2023), 2201107.
[21] D.C. Walter, D. Bredemeier, R. Falster, V.V. Voronkov, J. Schmidt, In 37-th European Photovoltaic Solar Energy Conference, 2020, p. 140. WIP-Munich.